Journal of Visualization, Vol. 10, No. 3 (2007)281-288

Regular Paper

Flow Visualization and Pressure Measurement in Micronozzles

Huang, C.*[1], Gregory, J. W.*[2] and Sullivan, J. P.*[3]

*1 School of Industrial Engineering, Purdue University, West Lafayette, Indiana 47907, USA.
E-mail: chihyung@purdue.edu
*2 Department of Aeronautics, US Air Force Academy, USAF Academy, Colorado 80840, USA.
*3 School of Aeronautics and Astronautics, Purdue University, West Lafayette, Indiana 47907, USA.

Received 7 December 2006
Revised 7 June 2007

Abstract : Micro devices have been widely used in aerospace engineering for years. Engineers are interested in applications of micro devices such as microjets, micro actuators, and micronozzles. The small size nozzles can be used for attitude adjustment and propulsion of micro-satellites or mini-spacecraft. In this paper, convergent-divergent micronozzles have been investigated at supersonic speed with various total pressures and Reynolds numbers. The throat of the micronozzle is 250 micron wide and the nozzle is designed as de Laval type. For the measurements, the Reynolds number at the throat varies from 1200 to 11000 and total pressure varies from 6 psia to 55 psia. Experimental results are obtained with pressure-sensitive paint for pressure measurement and schlieren imaging for flow visualization. Flow visualization is a challenge for conventional techniques due to the small length scales and small depth of the density gradient. A modified schlieren technique is used to increase the sensitivity by taking the ratio of wind-on and wind-off images. Pressure-sensitive paint is also used to obtain global pressure measurement of the flow field and to compare with the schlieren results.

Keywords : Visualization, Micronozzle, Pressure sensitive-paint, Schlieren.

1. Introduction

Micro-Electro-Mechanical-Systems (MEMS) devices are currently being used in daily life in products such as the micro-acceleration sensor in an automotive air bag system or microchannels used in the drug delivery systems. In addition to all the advantages and convenience of using MEMS devices, the physical phenomena of the small scales are significantly different from the normal scale and needs to be studied and understood. One of the micro devices that researchers have shown great interest in is the micronozzle, which involves a micro-scale, supersonic flow field. These small-size nozzles can provide thrust as low as 0.1 mN for thrust control with high accuracy. The physical characteristics of supersonic micronozzles have been investigated with numerical and experimental methods. But the extents of existing experimental approaches are limited, and most of the experimental results are restricted to the flow field outside of the micronozzle. Due to insufficient experimental results to validate the numerical methods, it is difficult to study the flow field with simulation approaches only.

When the scale for the nozzle geometry decreases, the most obvious change in the flow field is the dramatic decrease in the Reynolds number, which greatly increases the importance of viscous effects. For macro size nozzles, the Reynolds number based on the throat diameter is around 10,000 to 100,000 or even higher. However, for micro size nozzles, the Reynolds number is limited to a few thousand or even less than a few hundred. When the Reynolds number decreases, viscous effects begin to dominate the flow field. The Reynolds number is the ratio between inertial forces and

viscous forces and is defined as follows

$$\mathrm{Re}_t = \frac{\rho_t V_t D_t}{\mu_0} \tag{1}$$

where ρ is the density of the flow, V is the velocity, μ is the viscosity, and D is the characteristic length of the flow field, which is the throat height in nozzle flow. The nozzle flow at low Reynolds number conditions has been investigated with the Direct Simulation Monte Carlo methods, and the viscous layer was found to grow very rapidly from the sidewall and fill out the divergent section before the flow reached the nozzle exit (Zelesnik et al., 1994). The effect of a wall on the shock structure has been studied in micronozzle flow. There are differences between diffuse wall (non-slip) and specular wall (max-slip) conditions. The diffuse wall condition creates a weak but spreading shock wave inside the nozzle and makes the flow change to weak supersonic flow by the high viscous losses (Bouni et al., 2001). Experimental data has been acquired with the Electron-Beam technique to investigate the flow field inside the large size nozzle (Rothe, 1971). The results show that as the Reynolds number decreases, the viscous effect grows rapidly inside the nozzle and fills most of it. Temperature data indicates a shock-free viscous region inside the nozzle and a flow deceleration from supersonic to subsonic without shock wave interaction. Studies of the geometry and ambient pressure effects in micronozzle flow have performed. Separated flow is observed inside the nozzle. Because of the wide angle in the nozzle divergent section, the flow inside the nozzle acts as a free jet and reattaches to one side wall after passing through the throat. (Choudhuri et al., 2001). The shock wave has been studied at low pressure and high Knudsen number conditions where the shock became thickened and diffused (Kakkassery et al., 2002). Viscous effects in supersonic micronozzles have been investigated with numerical simulation and experimental measurement (Bayt et al., 1998). This study found that the viscous layer inside the micronozzle grows rapidly and fills the nozzle exit, creating a large deviation between numerical and experimental approaches for micronozzle research.

In order to obtain the detailed pressure data inside the micronozzle, an alternative experimental method is carried out by using pressure-sensitive paint (PSP). The PSP sensor has been applied in the MEMS measurement and successfully obtained the detailed information inside the MEMS device (Huang et al., 2002). In this paper, two experimental methods, PSP and a modified schlieren method, are used to obtain the flow field inside the micronozzles. The de Laval type micronozzle was used for the experiments with pressure varying from 1.5 to 55 psia and Reynolds number from 1200 to 11000. Modified schlieren results are also presented to compare with PSP results. In these experiments, the Reynolds number in the flow field varied from 1200 to 11000, which is a factor of two smaller than the large size nozzle. Due to the small Reynolds number, viscous effects can be expected to be much more dominant. Based on the test conditions and the pressure range for the micronozzle measurements, the flow inside the micronozzle can be assumed to vary only from continuum regime to slip-flow regime due to the relatively small Knudsen number.

2. Experimental Methods

2.1 Modified Schlieren Technique

Due to the difficulty of detecting the shock wave in micro flow field with schlieren technique, the modified schlieren technique is chosen to collect the flow visualization image in the micronozzle. For the modified schlieren technique, an imaging processing methodology a reference image is taken before the schlieren measurement. The reference image will be used for normalization with the traditional schlieren image, and the process can eliminate the noise from the back ground and the non-uniform illumination, and improve the contrast. To investigate the flow field in the micronozzle, the images collected with modified schlieren technique are used to help analysis the PSP data (Huang et al., 2007b).

2.2 PSP Technique

The PSP sensor is an optical-chemical sensor. It is constructed by embedding luminescent molecules into a binder, which can be a polymer or porous surface. With the excitation of a particular wavelength illumination, such as with a UV lamp or a blue/green LED, the luminescent molecules will be raised to higher energy state. To return to the original energy state, the luminophore will emit luminescence at longer wavelength. Because of the different wavelength between excitation and emission, the excitation light and emission light can be separated through the use of a low-pass optical filter in front of the light source and a high-pass optical filter in front of the photo detector. However, the luminescent intensity related to the energy transfer process will be affected by surrounding oxygen molecules through oxygen quenching. Oxygen quenching is a process in which the emission intensity is quenched by the existence of oxygen molecules in the nearby environment. Hence, as the oxygen concentration increases, the luminescent intensity decreases. Because of the fixed proportion of oxygen in the air, the relation of luminophore and oxygen molecules can also be used to measure the static pressure in the air. The Stern-Volmer equation is used for calibration with pressure and luminescent intensity and is described as follows:

$$\frac{I_{ref}}{I} = A(T) + B(T)\frac{P}{P_{ref}} \tag{2}$$

where I is the luminescent intensity, P is the static pressure, *ref* is the reference pressure measurement taken before the test, and A and B are the temperature-dependent coefficients that can be obtained through calibration.

After collecting the intensity of emission from the luminescent molecules with a photo detector, the luminescent intensity can be calibrated with pressure for pressure measurement. PSP can be used from the pressure range from vacuum to 2 atm with an accuracy of 1 mbar. The schematic of PSP measurement is shown in Fig. 1. PSP is a great experimental technique and has been successfully applied in wind tunnel experiments and unsteady flow measurements. (Engler et al., 2005; Gregory et al., 2005). Further details on pressure-sensitive paint theory and technique are given by Liu and Sullivan (Liu et al., 2005).

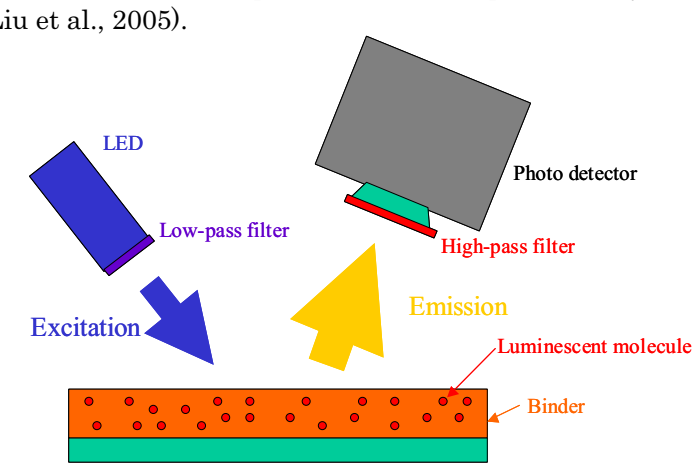

Fig. 1. Schematic of PSP measurement.

3. Experimental Setup

3.1 Micronozzle Device

The micronozzle is designed as a De Laval type nozzle. The micronozzle was machined from aluminum block with a high accuracy CNC machine. There are two large cavities at the nozzle inlet

and exit which act as reservoirs to set the pressure condition for operating micronozzle. There are two pressure taps installed in the micronozzle, one for the inlet reservoir and one for the exit reservoir, to monitor the pressure conditions. The geometry of the micronozzle is shown in Fig. 2. The throat height is 0.25 mm, the area ratio is 4.12, and the thickness is 2.5 mm. The nozzle is a De Laval type, with a convergent section length of 1.052 mm and a divergent section length of 3.175 mm. Completed details of the micronozzle geometry, along with nozzle height distribution and inviscid analysis, are available by Huang et al. (2002).

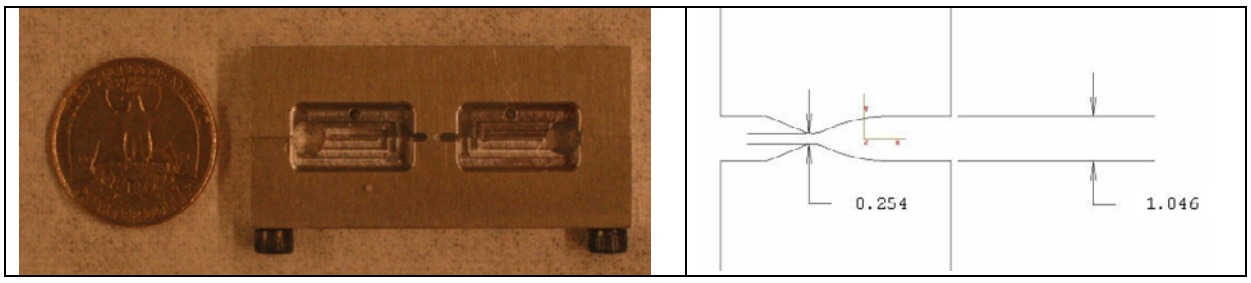

Fig. 2. Picture and schematic of micronozzle with units of millimeters.

3.2 Schlieren Setup

A single LED was used as the light source for the schlieren setup. A slit was placed in front of the LED to ensure a point light source, as needed. Two field lenses were set to make the light rays parallel passing though the flow field. A knife-edge was used to increase the contrast. A Photometrics 12-bit CCD camera (512 X 768 pixels) was used for collecting images. The exposure time for the CCD camera was set at 100 ms. The micronozzle entrance reservoir was connected to a compressed air supply, while the exit reservoir was connected to a vacuum tank to control the exit pressure. A Validyne CD15 differential pressure transducer (0-15 psid) was used for measuring the total pressure at micronozzle inlet. An Ashcroft test gauge (0-100 psia) was used for higher total pressure cases. An Omega px142 absolute pressure transducer was connected at the divergent section to monitor the pressure at the micronozzle exit. The micronozzle was installed with air flowing downwards, with the knife-edge set perpendicular to the flow direction. The schlieren setup for micronozzle is shown in Fig. 3.

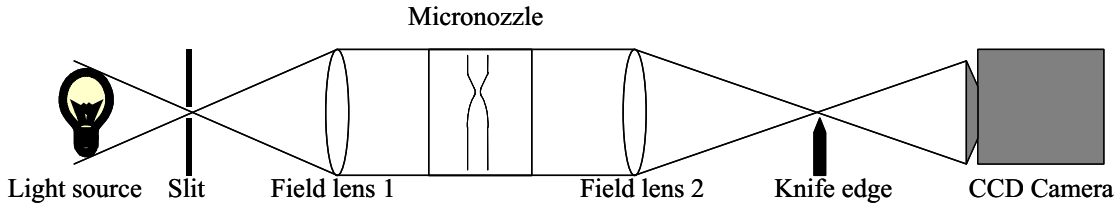

Fig. 3. Schematic of schlieren setup.

3.3 PSP Measurement Setup

The PSP measurement setup was the same as the schlieren setup except the field lenses and knife-edge were removed. A 550 nm high-pass filter was placed in front of the CCD camera to separate the excitation and emission signals. A 2-in UV lamp from ISSI was used for excitation. PtTFPP/TMSP was chosen as the PSP sensor for pressure measurement from 1 to 60 psia. The PSP of PtTFPP/TMSP was made by mixing 15 ml of TMSP solution with 7.5 mg of PtTFPP and 210 mg of polymer powder. The TMSP was 1-Trimethylsilypropyne obtained from Gelest, Inc. and the polymer powder was Poly(Methylsilsesquioxane) from Gelest, Inc. Because of the low viscosity of PSP paint, the paint can be spread and coated on the slide glass uniformly with a thickness of about 0.5 to 1 μm. Then the cover glass was attached and sealed with the micronozzle devices by cyanoacrylate glue. Figure 4 shows the experimental setup for PSP measurement. The micronozzle was oriented with the flow coming from the top to the bottom. Calibration of the paint was performed on a pixel-by-pixel basis to eliminate the effects of non-uniform sensitivity (Huang et al., 2007a). The PSP sensor with TMSP binder has a response time of 10ms (Liu et al., 2005).

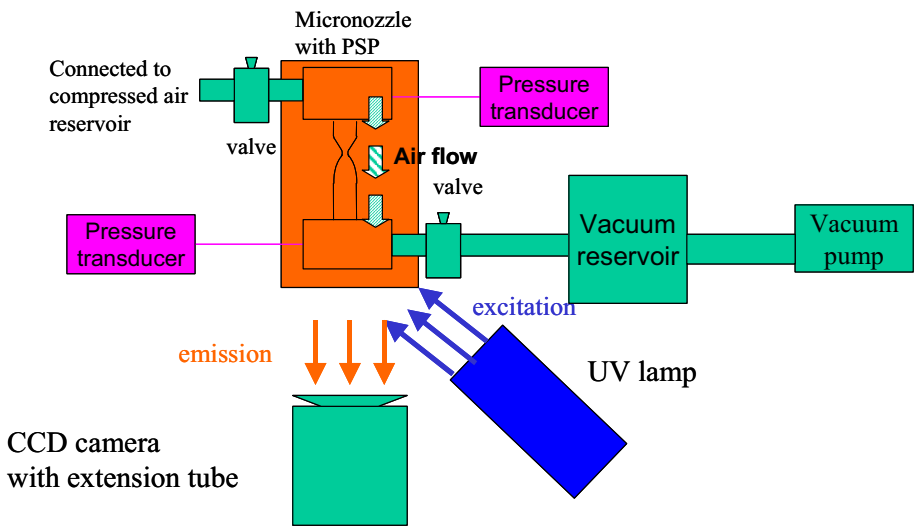

Fig. 4. Schematic of PSP setup.

4. Experimental Results

The experimental results include the modified schlieren results and PSP measurements for the micronozzle at high and low Reynolds number cases. The high and low Reynolds number conditions for all experiments are listed in Table 1.:

Table 1. Definition of high and low pressure conditions.

	Pressure at inlet	Pressure at exit	Reynolds number at throat	Pressure ratio (Pr)
High pressure case	22-55 psi	14.5 psi	4500-11000	1.5-3.8
Low pressure case	6 psi	1.58-4 psi	around 1200	1.5-3.8

4.1 Schlieren Results

The supersonic flow field of micronozzles is quite different between high and low Reynolds number conditions. At low Reynolds number conditions, the viscous effects increase dramatically and change the physical phenomena from high Reynolds number conditions. In micronozzle measurements, it is easy to reach low Reynolds number conditions because of the small scale; Reynolds number changes from 100,000 down to 1000. The flow visualization of the micronozzle is investigated with modified schlieren technique at different pressure ratios to study the shock wave behavior. All images shown here are the results from modified schlieren technique after taking a ratio with the wind-off image.

Figure 5 shows the images taken at higher pressure conditions for the high Reynolds number cases. The images were acquired while the pressure at the exit was held constant at ambient pressure, 14.5 psia, and the inlet pressure was changed from 22 to 55 psia to change the pressure ratio from inlet to exit from 1.5 to 3.8. At this pressure range, the Reynolds number for each test varied from 4500 to 11000. From images (a) to (d), it can be seen that the shock waves start from a pressure ratio greater than 2, and the shock waves are pushed downstream as the pressure ratio increases. Also, because of the sudden expansion after the throat in the micronozzle, the supersonic nozzle flow acts more like a supersonic free jet with a pattern of diamond-shape oblique shock waves, which attaches to the bottom wall. The shock wave behavior is very sensitive to the throat conditions. A slight change at the throat such as a small pressure change or a stagnation bubble will alter the shock wave pattern. Due to the instability of the shock wave movement, the shock wave jumps to the upper side of wall when the pressure reaches 3.8. In the shock wave images, only the first shock wave can be clearly identified. The shock waves after the first one are difficult to discern, most likely due to the large viscous effects.

Figure 6 shows the images for low-pressure conditions at the low Reynolds number conditions. The images were taken while the inlet pressure was held at 6 psia and the exit pressure was changed from 1.58 to 4 psia at a Reynolds number of 1200. It can be seen that the strength of shock waves decreases significantly and the shock waves move away from the bottom sidewall. This is because the viscous layers rapidly grow from the side wall due to the low Reynolds number condition, causing the shock waves to separate from the walls. However, even for the low Reynolds number conditions, shock wave patterns still can be seen when the pressure ratio is greater than 2.

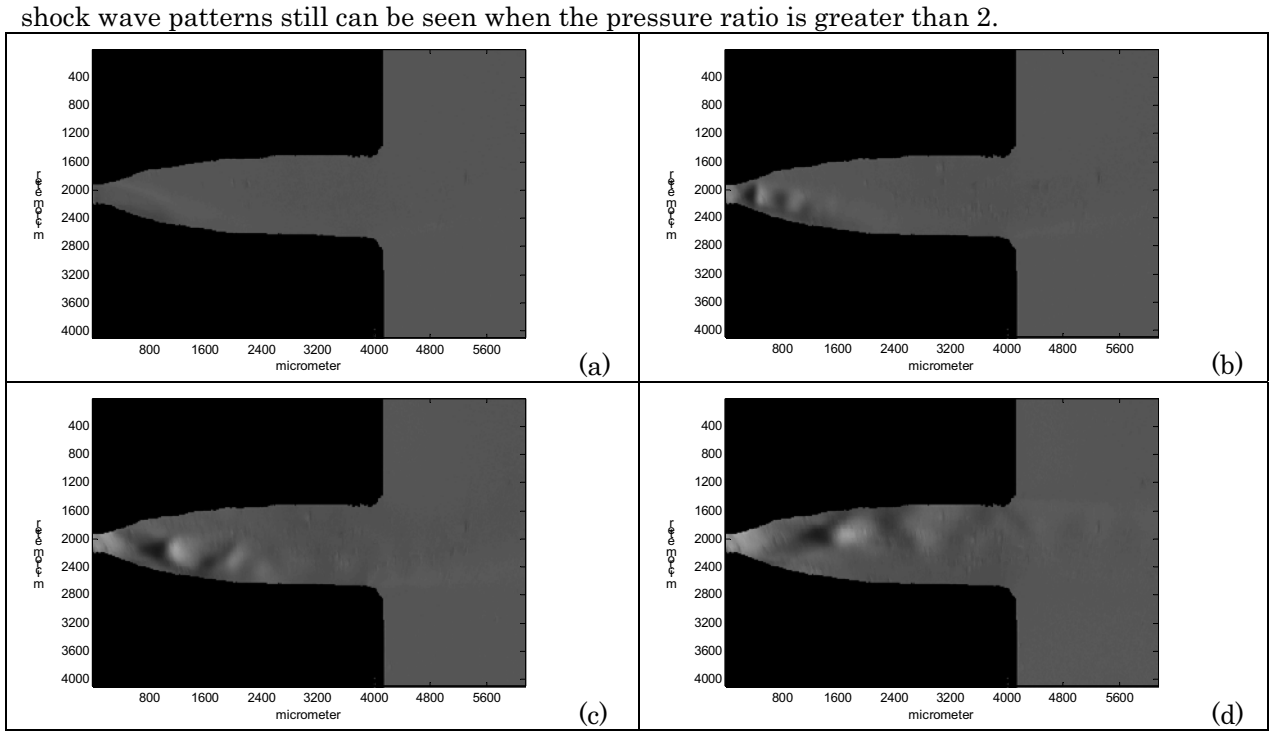

Fig. 5. Schlieren results of DL nozzle at high pressure condition. (a) Pr equals 1.5 (b) Pr equals 2 (c) Pr equals 3 (d) Pr equals 3.8.

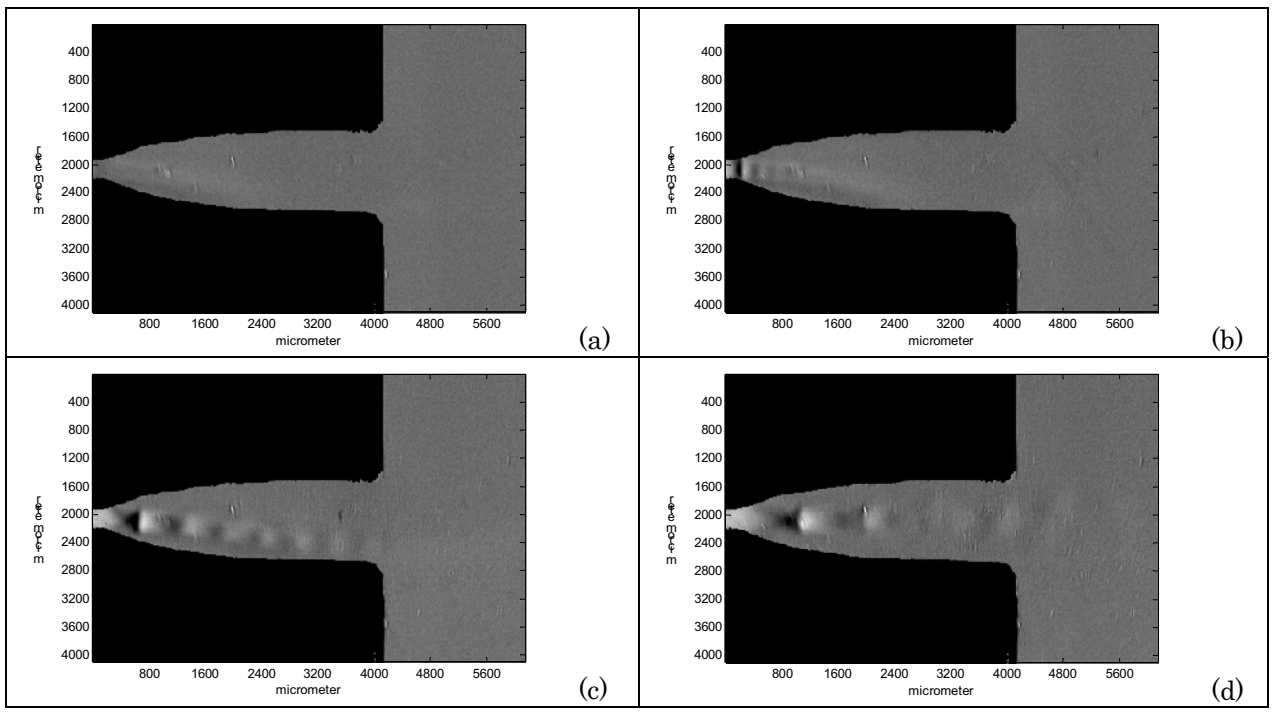

Fig. 6. Schlieren results of DL nozzle at low pressure condition. (a) Pr equals 1.5 (b) Pr equals 2 (c) Pr equals 3 (d) Pr equals 3.8.

4.2 PSP Measurement Results

Figure 7 shows the PSP measurement results of the micronozzle at the high-pressure conditions. Figure 7(a) shows the pressure distributions along the centerline of the micronozzle starting from the throat at different pressure ratios. Figure 7(b) shows the pressure map of the micronozzle at a pressure ratio of 3.8. The pressure jump from the shock wave appears in the pressure map as a red region in the divergent section. However, only one clear shock wave can be identified in the pressure map; the shock wave pattern after the first shock wave can not be seen here. A gradually increasing pressure region is located behind the shock wave due to viscous effects.

Figure 8 shows the PSP measurement results at low-pressure conditions. Figure 9 shows the modified schlieren image at a pressure ratio of 3.8 at high and low pressure conditions to compare with the pressure maps from PSP results. For the low-pressure cases, there are no shock waves detected in the PSP results, neither in the pressure distributions nor the pressure map. However, in the modified schlieren results in Fig. 9(b), a shock wave pattern can be seen. Although there are shock waves detected by modified schlieren results, the interaction of the shock wave with the thick laminar viscous layer will form a series of compression waves as λ-like shock waves. The series of compression waves will raise the pressure gradually instead of as a pressure jump as shown in the PSP data of the low-pressure cases. This phenomenon will make the pressure change from shock waves at the low Reynolds number condition differ from the high Reynolds number condition.

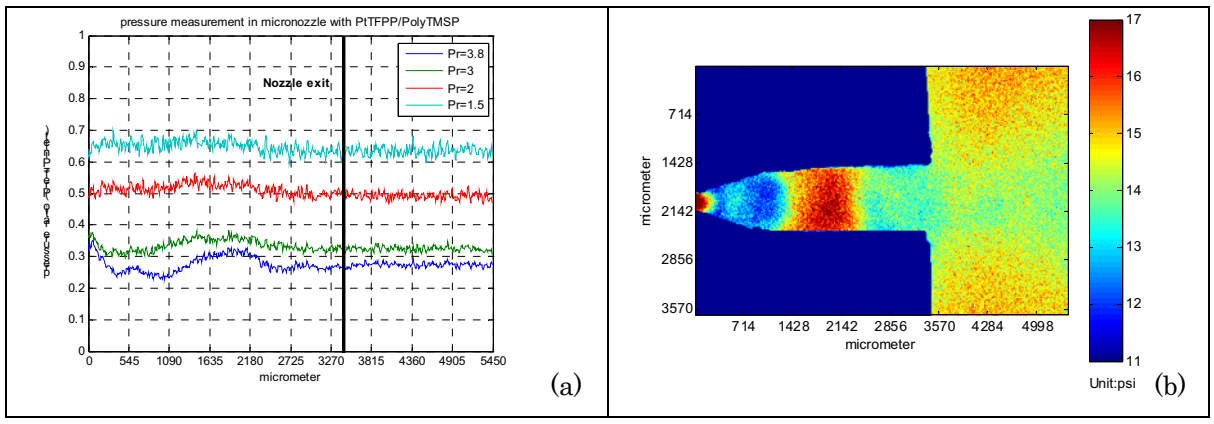

Fig. 7. (a) High pressure measurement with PSP (b) Pressure map of micronozzle at Pr equal to 3.8.

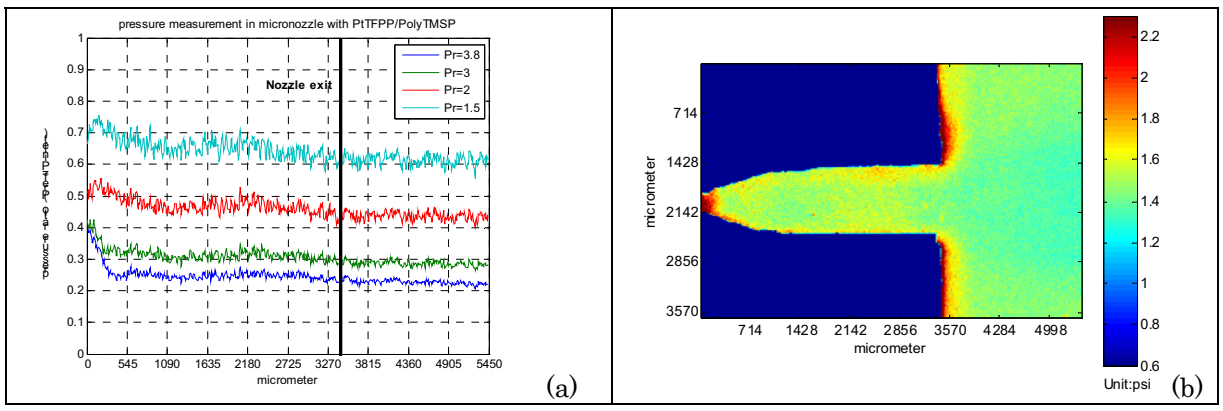

Fig. 8. (a) Low pressure measurement with PSP (b) Pressure map of micronozzle at Pr equal to 3.8.

5. Conclusions and Discussions

Micronozzles have been investigated with a modified schlieren technique and pressure-sensitive paint with the Reynolds number varied from 1200 to 11000. The spatial resolution in the PSP

measurement is as good as 7 μm. Different experimental methods have been used to compare the experimental results. At the high-pressure condition, the schlieren measurements show the clear shock wave pattern inside the divergent section of the micronozzle. Similar results can also be found in the pressure data from the PSP measurements. However, at low-pressure conditions, the shock waves that appear in modified schlieren results can not be detected in the PSP results. The reason for that is due to the thick viscous layer growing from the sidewall in the micronozzle as the low Reynolds number effect in low-pressure measurement. The shock waves interact with the laminar boundary layer to induce a series of compression waves and a λ- shock wave. The pressure gradually increases when passing through the λ shock structure (Bertin, 2001). Instead of showing a pressure jump pass through a shock wave, the pressure changes gradually as shown in the PSP data for laminar boundary interaction at the low-pressure condition.

References

Bayt, R. L. and Breuer, K. S., Viscous Effects in Supersonic MEMS-fabricated micronozzles, 3rd ASME Microfluid Symposium (Anaheim, CA.), (1998).
Bertin, J. J., Aerodynamics for Engineers, 4th Edition, (2001), Prentice Hall, NJ.
Buoni, M., Dietz, D., Aslam, K. and Subramaniam, V. V., Simulation of Compressible Gas Flow in a Micronozzle, 35th AIAA Thermophysics Conference (Anahiem, CA.), AIAA-2001-3073 (2001).
Choudhuri, A. R., Baird, B., Gollahalli, S. R. and Schneider, S. J., Effects of Geometry and Ambient Pressure on Micronozzle Flow, 37th AIAA/ASME/SAE/ASEE Joint Propulsion Conference and Exhibit (Salt Lake City, Utah), AIAA-2001-3331 (2001).
Engler, R. H., Fey, U., Henne, U., Klein, Chr. and Scahs, W. E., Quantitative Wind Tunnel Studies Using Pressure- and Temperature Sensitive Paints, Journal of Visualization, 8-3 (2005), 277-284.
Gregory, J.W., Sullivan, J.P. and Raghu, S., Visualization of Jet Mixing in a Fluidic Oscillator, Journal of Visualization, 8-2 (2005), 169-176.
Huang, C.-Y., Sakaue, H., Gregory, J. W. and Sullivan, J. P., Molecular Sensors for MEMS, 40th Aerospace Sciences Meeting & Exhibit (Reno, NV.), AIAA-2002-0256, (2002).
Huang, C.-Y., Gregory, J. W. and Sullivan, J. P., Microchannel Pressure Measurements Using Molecular Sensors, Journal of Microelectromechanical Systems, (2007a) (in press).
Huang, C.-Y., Gregory, J. W. and Sullivan, J. P., Modified Schlieren Technique for Micro Flow Visualization, Measurement Science and Technology, 18 (2007b), N32-N34.
Kakkassery, J.K., Sujith, R.I. and Kurian, J., On the Breakdown of Continuum and Shock Formation in Low-density Flows, Vacuum, 65 (2002), 45-50.
Liu, T. and Sullivan, J. P, Pressure and Temperature Sensitive Paints, (2005), Springer-Verlag, Berlin Heidelberg, Germany.
Rothe, D. E., Electron-Beam Studies of Viscous flow in Supersonic Nozzles, AIAA Journal, 9-5 (1971), 804-811.
Settles, G. S., Schlieren and Shadowgraph Techniques, (2001), Springer-Verlag, New York.
Zelesnik, D., Micci, M. M. and Long L. N., Direct Simulation Monte Carlo Model of Low Reynolds Number Nozzle Flows, Journal of Propulsion and Power, 10-4 (1994), 546-553.

Author Profile

Chihyung Huang: He received his B.S. and M.S. degrees in Aerospace Engineering from Tamkang University, Taiwan in 1995 and National Cheng Kung University, Taiwan 1997. Now he received his Ph.D. in School of Aeronautics and Astronautics at Purdue University. His current research interest is to apply PSP measurements in micro devices such as micronozzle, microjet, microchannel, and microturbine. He is now working as postdoctoral fellow in School of Industrial Engineering at Purdue University.

James W. Gregory: He received his Ph.D. (2005) and M.S. (2002) in Aeronautics and Astronautics from Purdue University, and a Bachelor of Aerospace Engineering from Georgia Tech in 1999. He is an NRC Postdoctoral Research Fellow at the US Air Force Academy. His work involves development of pressure-sensitive paint for unsteady aerodynamic applications, as well as the development of plasma actuators and fluidic oscillators as flow control actuators. He has been honored with the AIAA Wright Brothers Graduate Award (2005), the Boeing Engineering Student of the Year Award (2006), and first place in the AIAA National Student Paper Competition (2004).

John P. Sullivan: He received his B.S. in mechanical and aerospace sciences with honors from the University of Rochester in 1967, MS in 1969 and ScD in 1973 in aeronautical engineering from the Massachusetts Institute of Technology. Professor Sullivan has been a faculty member in the School of Aeronautics and Astronautics at Purdue since 1975, served as the director of the Aerospace Sciences Laboratory from 1983-1995, Head of the School from 1993-1998, and is Director of the Center for Advanced Manufacturing since 2004. His research interests include experimental aerodynamics, as well as advanced measurement techniques in fluid dynamics.